Proceedings of the ASME 2020
International Design Engineering Technical Conferences & Computers and Information in Engineering Conference
IDETC-CIE 2020
August 16-19, St. Louis, MO, USA

IDETC-CIE 2020-22241

INVARIANT MANIFOLDS IN HUMAN JOINT ANGLE ANALYSIS DURING WALKING GAIT.

Sandesh G. Bhat[1], Thomas G. Sugar[1,2], Sangram Redkar[1]

[1]Arizona State University, Mesa, Arizona, U.S.A.
[2]ASME Fellow

ABSTRACT

The complex dynamics of human gait is yet to be completely understood. Researchers have quantified stability of walking gait using Floquet multipliers as well as Lyapunov exponents. In this article, we utilize the techniques and tools from dynamical system theory and invariant manifolds to map the gait data onto a time invariant representation of a dynamical system. As an example, the complex behavior of the joint angle during walking was studied using a conformal mapping approach that transformed the time periodic system into a time invariant linear system. Time-delay embedding was used to reconstruct the dynamics of the original gait system with time series kinematic data. This minimal realization of the system was used to construct a Single Degree of Freedom (SDOF) oscillator. The time evolution of the linear oscillatory system was mapped back using the conformal mapping derived using Lyapunov-Floquet Theory. This algorithm was verified for walking gait kinematics data for two healthy human subjects. A comparison was drawn between the phase space behavior of the original time periodic system and the remapped time invariant system. The two systems showed good correlation. The algorithm resulted in a well correlated phase space representation.

Keyword: Biomechanics; Computational Dynamics of Bio-Mechanical and Biological Systems; Dynamics.

1. INTRODUCTION

Dynamics of human walking gait has been a topic of investigation since 1951 [1]. If properly understood, novel discoveries and theories in the field of prostheses, orthoses and rehabilitation can be realized. A broad range of techniques have been applied to analyze human gait. As stated in [2], the traditional way of analyzing gait cycles was to map data for a small number of gait cycles, time- normalize them to gait percentages and average the data for multiple gait cycles. While this method is useful for analyzing data for a general population, it is ineffective in answering questions about the dynamics or control of an individual's gait.

Dynamical system theory (DST) is the field of mathematics that deals with the behavior of dynamical systems. In the 1990's, Major applications involved classification of abnormal gait patterns [3]–[5]. Wagenaar et. al. described the role of DST in the investigation of control parameters as a necessary pre-requisite [6]. Researchers have also worked on generating a dynamic system model based control in gait applications [7], [8]. Morris et. al. achieved a successful simulation of a 5-link bipedal robot gait using invariant manifolds [8]. Frank et. al. applied time delay embedding, a technique from DST, in their activity recognition system [9]. Some researchers applied topological analysis techniques to recognize periodic motion in human beings [10]. In [11], Perc studied the human gait time series and concluded that the human gait was a deterministic chaotic system. In their article [12], Miller et. al. investigated a process to determine the presence of chaos in gait. In [13], [14], researchers studied the complex or irregularly periodic behavior of the human gait but did not term it as chaotic. All the above examples showed there was no single consensus in

the scientific community over the type of dynamical system that represents human gait.

In order to analyze human walking gait, we applied the tools from DST and invariant manifolds. The human gait behavior was assumed to be periodic rather than a chaotic system, or even a quasi-periodic system as it introduces complexity in the analysis of the said system. Hence, a conformal map was developed to transform the complex behavior of the human gait system onto a much simpler time invariant linear dynamical system as discussed in the following section.

2. CONCEPTS

2.1 Dynamical System Theory in Gait Application:

The human gait system is dynamically complicated to analyze. Researchers have used different ways to approach the problem [6]-[17] while approximating the behavior of the system. Although human gait is not purely periodic, an assumption can be made, and the human gait system can be analyzed as a periodic system. Such a periodic system can be represented as

$$\dot{x} = A(t)x + E(x,t) + F(t),\ x \in \mathbb{R}^n \tag{1}$$

where $A(t)$ and $E(x,t)$ are T periodic i.e. $A(t) = A(t+T)$ and $E(x,t) = E(x,t+T)$. $E(x,t)$ represents the nonlinear part of the system. $F(t)$ represents the external force term [15]. The linear form of equation (1) without any force term is represented by

$$\dot{x}(t) = A(t)x(t) \tag{2}$$

Further analysis performed in this manuscript assumes human walking gait as a uniformly periodic linear system. No external forces are considered as the magnitude of forces in the direction of motion would be low.

2.2 Lyapunov-Floquet Theory:

For a given nth-order periodic system from equation (2):

$$\dot{x}(t) = A(t)x(t),\ x \in \mathbb{R}^n \tag{3}$$

the solution can be represented by

$$x(t) = \phi(t, t_0)x_0 \tag{4}$$

where $\phi(t, t_0)$ is the State Transition Matrix (STM) for the given system from time t_0 to t. Considering t_0 = 0,

$$\phi(t, 0) \equiv \phi_0(t) \tag{5}$$

Hence, for t_0 = 0, equation (4) becomes

$$x(t) = \phi_0(t)x_0 \tag{6}$$

It has also been established in literature that

$$\phi_0(t) = Q(t)e^{Rt} \tag{7}$$

where $Q(t)$ is a non-singular $n \times n$ periodic matrix with period T and R is a $n \times n$ finite constant matrix. The system is defined as T-periodic. Hence it follows that $\phi_0(t)$ is also periodic over T [15]–[17] i.e. $\phi_0(0) = \phi_0(T)$. If the initial conditions are defined as identity (i.e. $x_0 = I_{n\times n}$) then,

$$\phi_0(0)x_0 = x(0) \tag{8}$$

$$i.e.\ \phi_0(0) = I_{n\times n} \tag{9}$$

Therefore from equations (7) and (9) it is clear that

$$\phi_0(0) = Q(0) = I_{n\times n} \tag{10}$$

Since $Q(t)$ is periodic over T, $Q(T) = I_{n\times n}$. Hence, from equation (7), $\phi_0(T)$ is a constant.

$$\text{i.e. } \phi_0(T) = e^{RT} \tag{11}$$

This representation of the state transition matrix at period T is also known as the Floquet Transition Matrix (FTM). Let the FTM be denoted by $\Phi(T)$ i.e. $\Phi(T) = \phi_0(T) = e^{RT}$. At time t = T, equation (4) becomes $x(T) = \Phi(T)x_0$. Therefore, it holds that to calculate the FTM, one can use the values of the state variables at t = 0 and t = T.

$$i.e.\ \Phi(T) = x(T)x_0^{-1} \tag{12}$$

The above analysis holds for a continuous system. It is applicable to a discrete system, but it is difficult to obtain the original system's behavior using a one-dimensional time series. To analyze a scalar one-dimensional time series, the data is embedded into multiple dimensions using time-delay embedding.

2.3 Time-Delayed Embedding:

A time series can be said to be a projection of unobserved internal elements of a dynamical system onto the real domain [18]. Such a projection may be nonlinear and can be affected by the original system's internal variables. This leads to distortion in the output making it impossible to reconstruct the phase space of the original system. To ensure similarity in properties between the actual system and the constructed system using a time series, the data is embedded. H. Kantz et al. [18] describe embedding as a mapping operation where embedding a smooth manifold G into $\mathbb{R}^m$ is defined as a map F which is a one-to-one C^1 map with a Jacobian $DF(t)$ which has full rank everywhere. Taken's time delay embedding theorem [19] uses a delay vector to reconstruct the phase space. The delay vector is of the type $\left(s(x_n), s\left(F(x_n)\right), s\left(FoF(x_n)\right), \dots\right)$ where x_n is the state vector and F is the map represented by $x_{n+1} = F(x_n)$. Let this time delay be denoted by τ. The value of τ cannot be large. A large τ will lead to a complicated reconstruction of the attractor system. It must be noted that a reasonable value of τ has no effect on the underlying mathematics of the system. There is no proven method to find an optimum value of τ [18].

The embedding dimension can be found out by performing a Principal Component Analysis (PCA) on the data. Also known as Singular Value Decomposition (SVD), it is a technique to characterize the data into its most important components in the embedding space $\mathbb{R}^m$ [18]. SVD was used to find a square matrix consisting of its principal values. The diagonal elements were divided by their sum to calculated s. The value of m was found when the value of s less than or equal to the threshold value. The value of m can be larger than the optimal value, but the resulting system will reflect the underlying properties of the actual system.

2.4 Invariant Manifold:

An Invariant Manifold is a geometric construct that is not affected by the flow of the system. Mathematically, a manifold is defined as a subset $M \subset \mathbb{R}^n$ which can be locally represented as a graph of a smooth function. Such a manifold is said to be invariant if under the effect of a flow F, for every $x \in M$, $F_t(x) \in M$ for a small $t > 0$. It helps to define a co-ordinate transformation, or a mapping, that represents an invariant manifold locally. Let such a transformation of co-ordinate system be described by $\psi: V \to \mathbb{R}^k \times \mathbb{R}^{n-k}$ in the neighborhood $V \subset \mathbb{R}^n$ [8]. Let the local co-ordinate system of ψ be defined as the z domain (where z is two dimensional). In the case of this manuscript, the transformation was defined as $x(t) = Q(t)z(t)$, where $x(t)$ is the original system and $z(t)$ is the transformed system. Since the goal was to map the gait system as a SDOF oscillator, the $z(t)$ system was designed to have an elliptical phase space response.

With the concepts defined, we applied them to walking gait data collected from healthy human subjects. The next section describes the analysis of a SDOF oscillator that can be mapped back to the original system.

3. APPLICATION

3.1. Data Collection:

Two subjects were asked to walk on a treadmill at a normal walking speed of 1.2 ms^{-1}. These subjects were equipped with a harness (to prevent fall related injury) and motion capture markers. The subjects walked for 3 minutes continuously. Data for the right leg was measured for each subject using a Vicon motion capture system with a sample rate of 100 Hz. A Newington-Helen Hayes model was used. The data was then filtered using a low-pass Butterworth filter with cutoff frequency of 10 Hz. Only the data with minimal stride-to-stride variability was considered for the process detailed below. The experimental protocol was reviewed by Arizona State University's Institutional Review Board (STUDY 00009416).

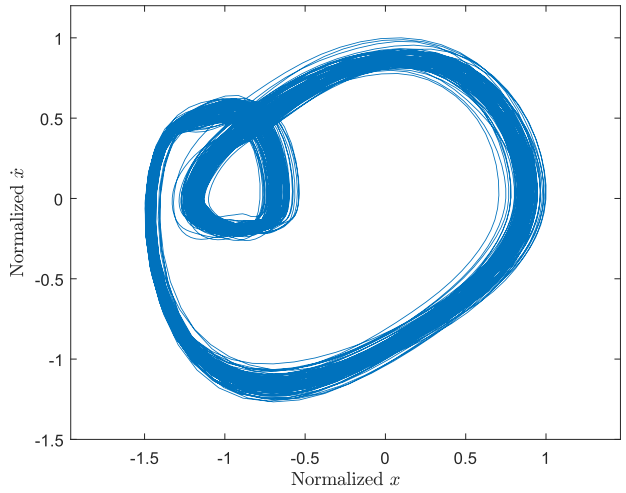

FIGURE 1. PHASE PLOT FOR SUBJECT A'S KNEE ANGLE DATA.

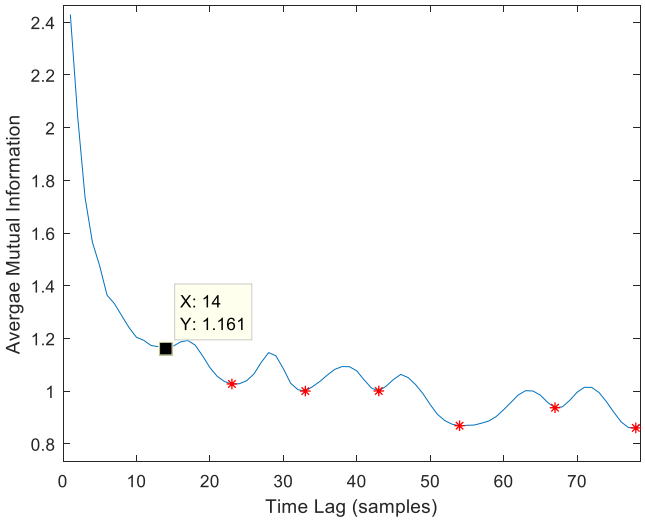

FIGURE 2. AVERAGE MUTUAL INFORMATION VS TIME LAG PLOT FOR SUBJECT A. BLUE LINE INDICATES THE AMI AND RED ASTERISKS INDICATE THE MINIMA.

3.2. Mapping and Re-Mapping:

All the analysis and data processing were done in MATLAB 2018a. The collected data were prepared for analysis by segmenting the data at heel strike events. A derivative of the data was calculated (i.e. angular velocity). The data was shifted by its value at the point its derivative was maximum. Then both the data and its derivative, were scaled with their maximum value to satisfy the initial condition of identity. The angular rotation and angular velocity data, for the ankle and knee joints, formed the actual time series $x(t)_{2\times n}$. In order to calculate the time-delay necessary to reconstruct the system, Average Mutual Information (AMI) was calculated for the data [20]. Time lag (τ) was selected to be the first minima of the resulting data as instructed in [18]. This data (represented by $x(t)_{2\times n}$) was two-dimensional time series. Phase space data was reconstructed using the original data ($x(t)_{2\times n}$) and the time-delayed versions of the same data ($x(t + n\tau)_{2\times n}$) [18], [21].

It was observed that the reconstructed system's stability varied with respect to the number of gait cycles used in the calculation of the embedding dimension. This was due to the varying time period for each gait cycle. Hence, a loop was run in order to find the optimum number of gait cycles that would lead to a simply stable reconstructed system. The termination condition for the loop was the value of FTM (i.e. $\Phi(T) = I$). An SVD method was used to determine the embedding dimension m. A new matrix was constructed using the time-delay and embedding dimension calculated above, which can be represented as $X_{2\times n\times m} = [x(t), x(t+\tau), x(t+2\tau), \ldots, x(t+(m-1)\tau)]$ where $0 \le t \le T$ and T is the gait

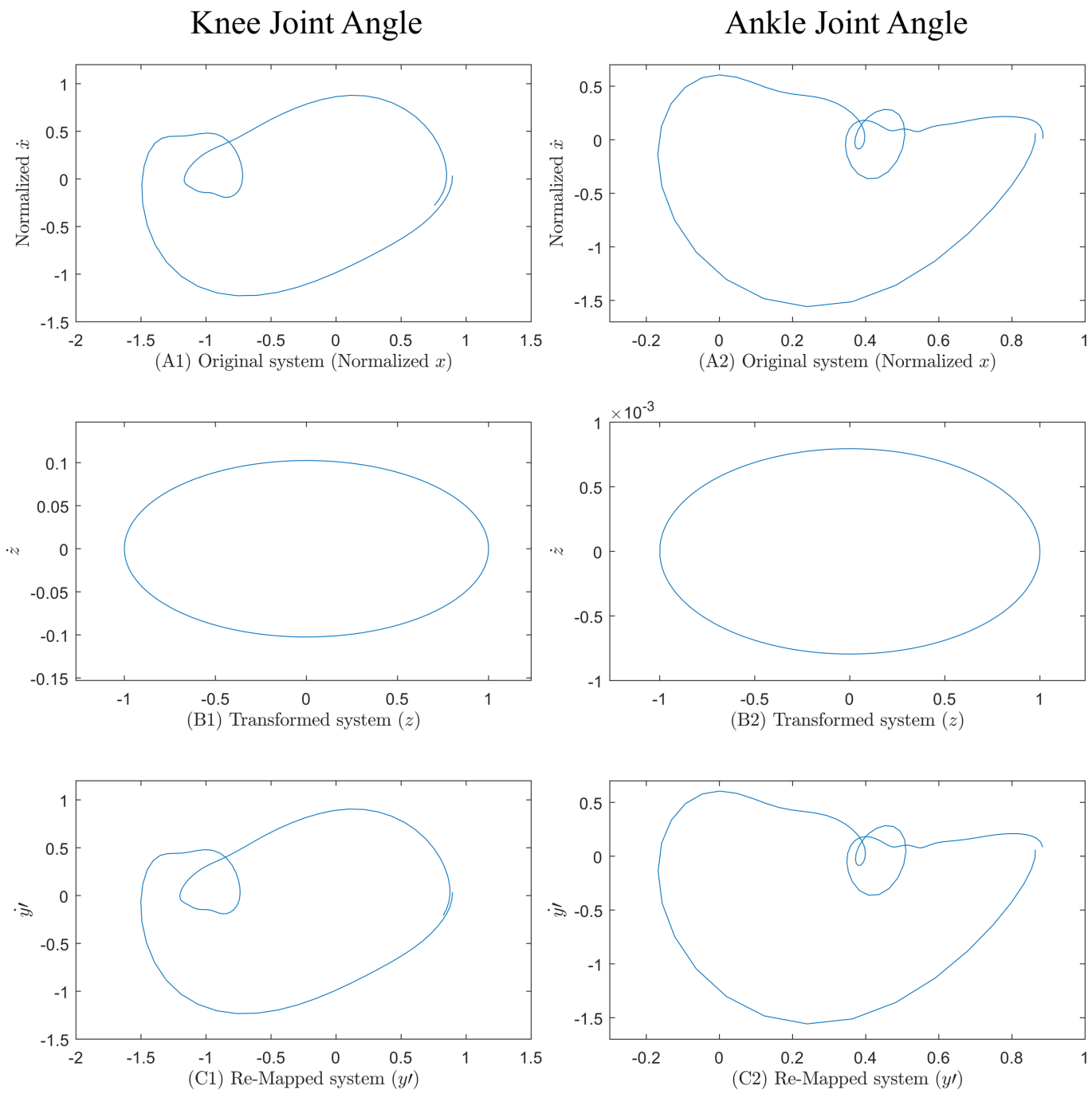

FIGURE 3. (A1, A2) THE ORIGINAL ANGLE PHASE PLOT, (B1, B2) THE RESPONSE OF THE CONFORMAL MAP GENERATED USING THE SYSTEM IN A1, A2 RESPECTIVELY, (C1, C2) THE TRANSFORMED SYSTEM USING THE RELATIONSHIP IN EQUATION (16)

cycle period. To calculate the FTM, data for the first ($t = 0$) and last ($t = T$) time steps were used (as in equation (12))

$$i.e.\,\Phi(T)_{2\times 2} = X(T)_{2\times m}(X(0)^{-1})_{m\times 2} \qquad (13)$$

The matrix $R_{2\times 2}$ (from equation (7)) was calculated by taking a matrix log (logm() in MATLAB) of $\Phi(T)_{2\times 2}$. Floquet exponents (L), i.e. the eigenvalues of $R_{2\times 2}$ were complex with a very small real part due to the conditions set on the embedding dimension.

The original time series was divided into two sets such that their initial conditions were [1,0] and [0,1] approximately and the sets had k gait cycles. These two sets were combined in order to form the data $y(t)_{2\times 2}$ where $0 \le t \le kT$. The initial condition of this time series was approximately the identity matrix,

$$i.e.\,y(0) \approx I_{2\times 2} \qquad (14)$$

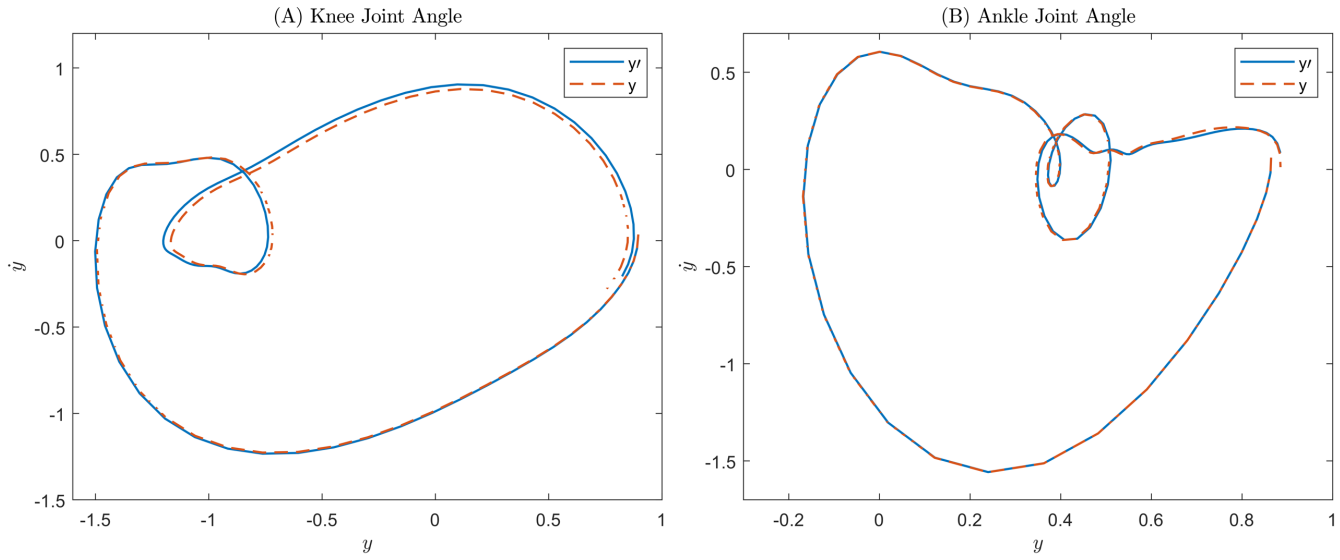

FIGURE 4. PHASE PLOT COMPARISON BETWEEN ORIGINAL DATA (DASHED ORANGE) AND REMAPPED DATA (BLUE) FOR ONE GAIT CYCLE (k = 1) FOR SUBJECT A

The STM $(\phi_0(t)_{2\times2})$ was calculated using the relationship in equation (6). which was used to calculate the $Q(t)$ matrix

$$i.e.\, Q(t)_{2\times2} = \phi_0(t)_{2\times2} \mathrm{e}^{-R_{2\times2}t} \tag{15}$$

The $Q(t)$ matrix was used to form a map to a new co-ordinate system z such that,

$$y(t) = Q(t)z(t) \tag{16}$$

The system in the $z(t)$ domain was defined as a simple linear oscillator with the squared Floquet exponent of the embedded system as the stiffness coefficient with zero damping.

$$i.e.\, \ddot{z} + L^2 z = 0 \tag{17}$$

The system was evaluated for $0 \leq t \leq kT$ (where k was the number of gait cycles considered for the analysis) with initial condition $z(0) = Q(0)^{-1}y(0)$ and then remapped to the $y(t)$ domain as $y'(t)$. $y(t)$ and $y'(t)$ were then compared to quantify the success of this method.

4. RESULT AND ANALYSIS

As stated in [2], human gait has been analyzed by averaging multiple gait cycles. Instead, our goal was to analyze and model an individual gait cycle. Hence, a deeper analysis on one subject's data was performed to allow for a deeper understanding of the algorithm. The selected subject was denoted subject A. The average gait cycle duration (T) for subject A was 116 samples (1.16 seconds). A phase space plot for subject A's knee angle is shown in Figure 1. Time delay

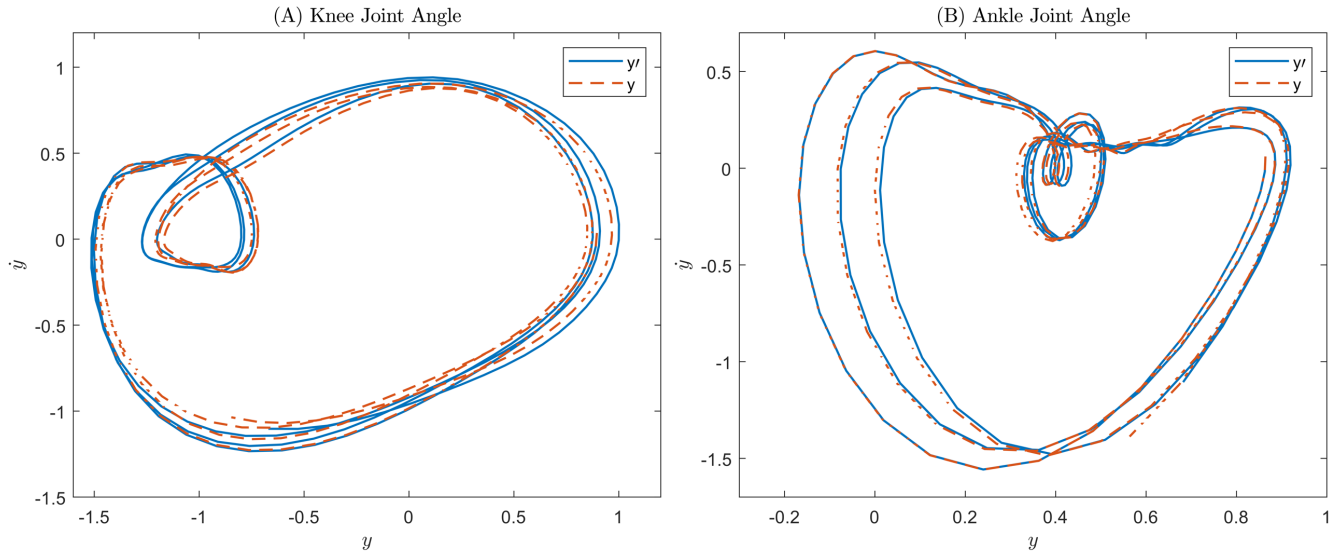

FIGURE 5. PHASE PLOT COMPARISON BETWEEN ORIGINAL DATA (DASHED ORANGE) AND REMAPPED DATA (BLUE) FOR 3 GAIT CYCLES (k = 3) FOR SUBJECT A

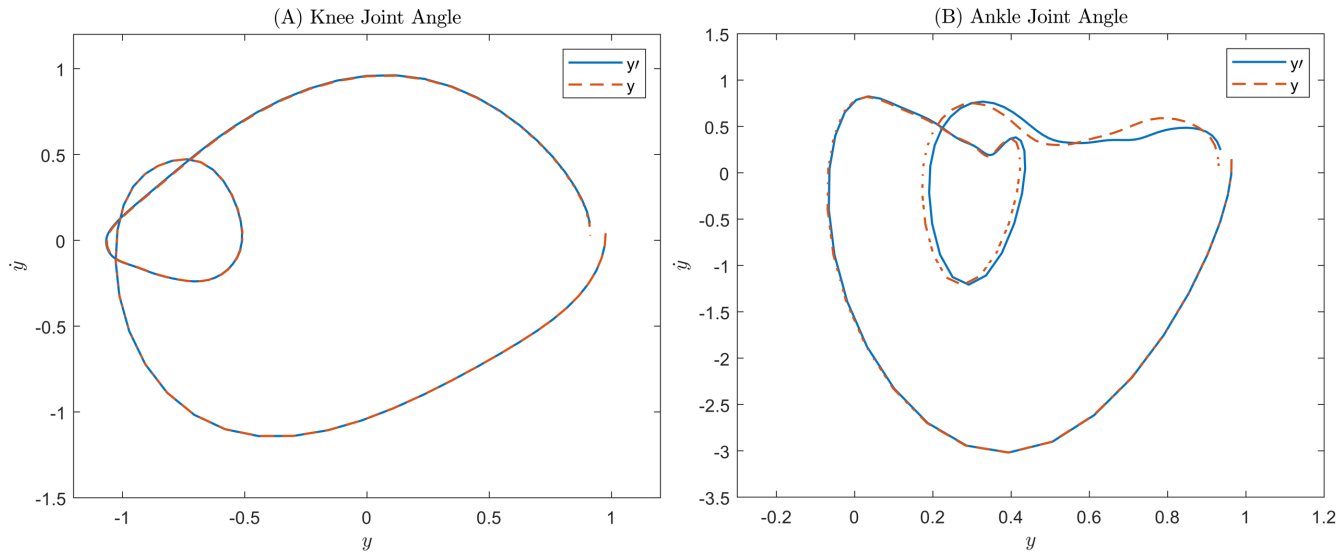

FIGURE 6. PHASE PLOT COMPARISON BETWEEN ORIGINAL DATA (DASHED ORANGE) AND REMAPPED DATA (BLUE) FOR ONE GAIT CYCLE (k = 1) FOR SUBJECT B

was calculated to be 14 samples (first minima as seen in Figure 2) using the mai.m function by A. Leontitsis [20]. This time delay was acceptable as it was just 12% of the time period of the data. As stated above, a large time delay might cause the reconstructed system to be different than the underlying system. Delaying the data with 14 samples would not cause the system properties to change. Next, the optimum number of gait cycles for the calculation of FTM was determined to be 33. Using SVD, the embedding dimension was found to be 8 with a criterion of $s < 0.02$. Using the time lag and embedding dimension, a system was reconstructed that had an FTM with eigenvalue $1.0016 \pm 0.1027i$ (absolute value 1.0069). This showed the reconstructed system was simply stable. The system had a Floquet exponent of $0.0068 \pm 0.1022i$ which was used to generate a map to the z-domain. The linear system formed using the Floquet exponent was:

$$\ddot{z} + 0.0105z = 0 \tag{18}$$

Similar values were calculated for subject A's ankle angle data.

Figure 3 shows the transformation procedure described above applied to subject A's knee and ankle angle data. Figure 3(A1, A2) show a normalized gait cycle for the original system. Figure 3(B1, B2) show the phase space response of the linear system generated by the conformal mapping procedure. A single gait cycle in the original system formed a part of the phase space portrait in the z domain. When this section of the $z(t)$ system was remapped back to the joint phase space, the behavior was as in Figure 3(C1, C2).

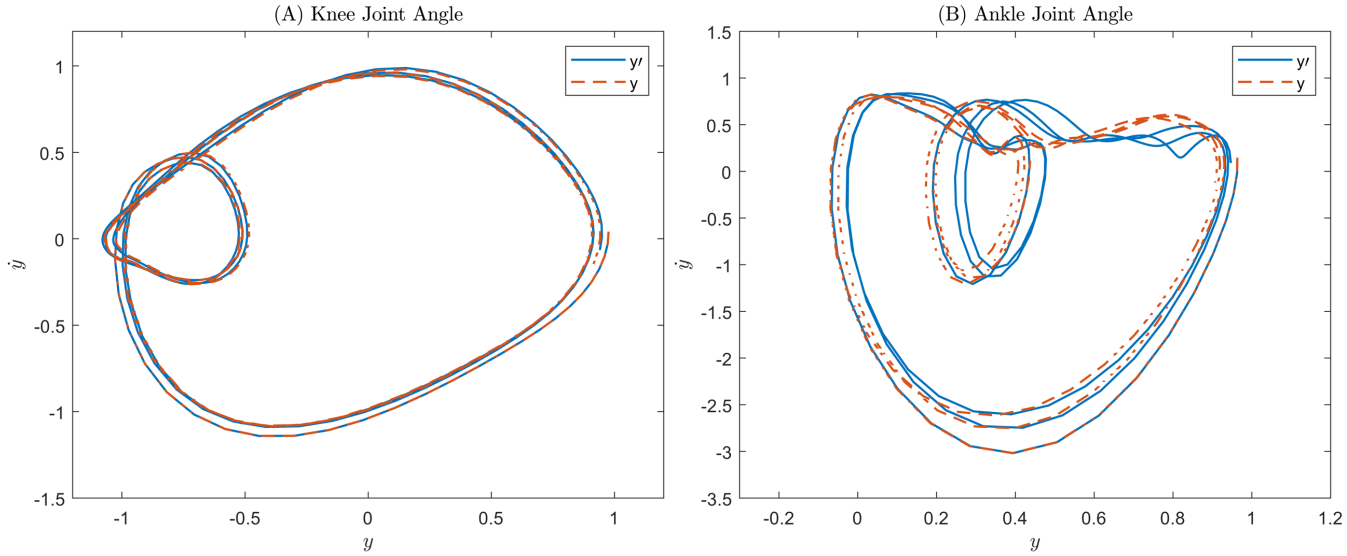

FIGURE 7. PHASE PLOT COMPARISON BETWEEN ORIGINAL DATA (DASHED ORANGE) AND REMAPPED DATA (BLUE) FOR 3 GAIT CYCLES (k = 3) FOR SUBJECT B

The remapped system's response roughly matches the actual system's response. Figure 4 and 5 show the phase space response of the original system as compared to the remapped system's response for subject A and Figure 6 and 7 display the same data for subject B. As can be seen in Figure 4(A, B) and Figure 6(A, B), the initial response of the $y'(t)$ system was similar to the original system ($y(t)$). There were a few instances where the remapped system's response was different from the original system's response, but these differences were minor. Figure 5(A, B) and Figure 7(A, B) show the responses of the two systems after 3 gait cycles for each case. There were some deviations from the original system over three gait cycles. These deviations were more apparent in some cases than the others (Figure 7A compared to Figure 7B). However, the remapped system still mimicked the general behavior of the original system in each case.

For a better match, the remapped system can be reinitiated, i.e. the $z(t)$ system can be integrated for only a couple gait cycles (kT samples) for a better correlated data. The result of this integration can be then remapped to the $y'(t)$ domain. It must be noted that the output of the algorithm is affected by the variability in the system. The success of the algorithm depends on the eigenvalue of the FTM matrix. Cases with eigenvalues closer to 1 showed better correlation between the original and remapped data. The eigenvalues were a metric to determine the stability of the system reconstructed using time-delayed embedding. The absolute value of the eigenvalues in case of subject A's knee angle were 1.0069 and that in case of subject A's ankle angle were 0.9992. For subject B, the values of the eigenvalue for the knee and ankle joint angles were 0.9960 and 0.9793 respectively. Out of the four cases displayed in Figures 5 and 7, subject B's knee joint angle plots (Figure 7 A) and Subject A's ankle joint angle (Figure 5 B) had the best correlation. This can be accounted to the eigenvalues for these cases being the closest to unity.

The z-domain response was observed to be different for each case. Even for the same subject, the value of the Floquet exponent was different for each joint, which dictated the response in the z-domain. It was noted that due to the initial condition of the normalized system being set to near identity, the initial condition for z and $\dot{z}$ was consistently close to [1, 0]. Hence the semi-major axis of the elliptical response was 1 and the semi-minor axis was determined by the imaginary part of the Lyapunov exponent (as seen in Figure 3B1 and 3B2). The results for subject A showed the possibility of using the discussed algorithm to map the complicated human gait system to a linear dynamical system. This reduces the order of the system. Since the mapped system was linear, a phase space controller such as the ones used in [22]–[24] could be easily applied to the linear system. The phase space controller applied to the linear system would in turn require lower computational power making the control aspect of any prostheses or rehabilitation device simpler. The real-time application of this algorithm is a subject of future research.

5. CONCLUSION

The results discussed in this article all point to the fact that human walking gait has an Invariant Manifold and it is possible to use this Manifold to obtain a time invariant form of the system. The complex behavior of the human gait system was mapped onto a linear SDOF oscillator using a conformal map generated by applying Lyapunov-Floquet Theory to the gait data. The order of the system was reduced to its minimum possible realization while retaining the dynamical properties of the original system. It was shown that the behavior of the system in the mapped domain (z-domain) had a direct effect on the remapped system (y'-domain). We believe a similar process can be applied to other joints in periodic/ quasi-periodic motions in the human body in varying conditions. The next step would be to apply the algorithm onto human gait under different external impetus (e.g. Incline/decline walking, varying speed of walking, running, etc.).

AKNOWLEDGEMENTS

We would like to thank Arizona State University for supporting this venture.

REFERENCES

[1] B. Bresler and F. R. Berry, *Energy and power in the leg during normal level walking*. Prosthetics Devices Research Project, Institute of Engineering Research~…, 1951.

[2] J. B. Dingwell and J. P. Cusumano, "Nonlinear time series analysis of normal and pathological human walking," *Chaos An Interdiscip. J. Nonlinear Sci.*, vol. 10, no. 4, pp. 848–863, 2000.

[3] K. M. Newell, R. E. A. van Emmerik, D. Lee, and R. L. Sprague, "On postural stability and variability," *Gait Posture*, vol. 1, no. 4, pp. 225–230, 1993.

[4] R. E. A. Van Emmerik, R. C. Wagenaar, and E. C. Wolters, "Dynamics of movement coordination in Parkinson's disease," in *Mental dysfunction in Parkinson's disease*, ICG Printing, Dordrecht, The Netherlands, 1993, pp. 69–91.

[5] R. C. Wagenaar and W. J. Beek, "Hemiplegic gait: a kinematic analysis using walking speed as a basis," *J. Biomech.*, vol. 25, no. 9, pp. 1007–1015, 1992.

[6] R. C. Wagenaar and R. E. A. van Emmerik, "Dynamics of pathological gait," *Hum. Mov. Sci.*, vol. 13, no. 3–4, pp. 441–471, 1994.

[7] M. Anand, J. Seipel, and S. Rietdyk, "A modelling approach to the dynamics of gait initiation," *J. R. Soc. Interface*, vol. 14, no. 128, p. 20170043, 2017.

[8] B. Morris and J. W. Grizzle, "Hybrid invariant manifolds in systems with impulse effects with application to periodic locomotion in bipedal robots," *IEEE Trans. Automat. Contr.*, vol. 54, no. 8, pp. 1751–1764, 2009.

[9] J. Frank, S. Mannor, and D. Precup, "Activity and gait recognition with time-delay embeddings," in *Twenty-*

Fourth AAAI Conference on Artificial Intelligence, 2010.

[10] S. Hidaka and T. Fujinami, "Topological similarity of motor coordination in rhythmic movements," in *Proceedings of the Annual Meeting of the Cognitive Science Society*, 2013, vol. 35, no. 35.

[11] M. Perc, "The dynamics of human gait," *Eur. J. Phys.*, vol. 26, no. 3, p. 525, 2005.

[12] D. J. Miller, N. Stergiou, and M. J. Kurz, "An improved surrogate method for detecting the presence of chaos in gait," *J. Biomech.*, vol. 39, no. 15, pp. 2873–2876, 2006.

[13] N. Scafetta, D. Marchi, and B. J. West, "Understanding the complexity of human gait dynamics," *Chaos An Interdiscip. J. Nonlinear Sci.*, vol. 19, no. 2, p. 26108, 2009.

[14] L. M. Decker, F. Cignetti, and N. Stergiou, "Complexity and human gait," *Rev. Andaluza Med. del Deport.*, vol. 3, no. 1, pp. 2–12, 2010.

[15] S. C. Sinha, R. Pandiyan, and J. S. Bibb, "Liapunov-Floquet transformation: Computation and applications to periodic systems," 1996.

[16] H. D'Angelo, "Linear time-varying systems: analysis and synthesis," 1970.

[17] C. Chicone, *Ordinary differential equations with applications*, vol. 34. Springer Science & Business Media, 2006.

[18] H. Kantz and T. Schreiber, *Nonlinear time series analysis*, vol. 7. Cambridge university press, 2004.

[19] F. Takens, "Detecting strange attractors in turbulence," in *Dynamical systems and turbulence, Warwick 1980*, Springer, 1981, pp. 366–381.

[20] A. Leontitsis, "Mutual Average Information." [Online]. Available: https://www.mathworks.com/matlabcentral/fileexchange/880-mutual-average-information.

[21] P. T. Chinimilli, "Human Activity Recognition and Control of Wearable Robots," Arizona State University, 2018.

[22] P. New, C. Wheeler, and T. Sugar, "Robotic hopper using phase oscillator controller," in *ASME 2014 International Design Engineering Technical Conferences and Computers and Information in Engineering Conference, IDETC/CIE 2014*, 2014.

[23] J. Kerestes, T. G. Sugar, and M. Holgate, "Adding and subtracting energy to body motion: Phase oscillator," in *ASME 2014 International Design Engineering Technical Conferences and Computers and Information in Engineering Conference*, 2014.

[24] T. G. Sugar *et al.*, "Limit cycles to enhance human performance based on phase oscillators," *J. Mech. Robot.*, vol. 7, no. 1, 2015.